ORIENTAL JOURNAL OF CHEMISTRY
An International Open Access, Peer Reviewed Research Journal
www.orientjchem.org
ISSN: 0970-020 X
CODEN: OJCHEG
2026, Vol. 42, No.(2):
Pg. 626-638

Process Optimization and Physicochemical Evaluation of Activated Carbons Produced from Shea Nut Shells (*Vitellaria paradoxa*)

SIRATA IBRAHIMA FRANCIS SORO[1]*,AFFOUÉ TINDO SYLVIEKONAN[1], IGNACE CHRISTIANM'BRA[1], KOFFI SIMÉONKOUADIO[1,3], TANOÉ LUCIENAKETCHI[1,2], DANIEL YANNICK DJÈ[1] and LYNDA EKOU1,TCHIRIOUA EKOU[1]

[1]Laboratoire de Thermodynamique et Physico-Chimie du Milieu (LTPCM), Unité de Formation et de Recherche SciencesFondamentales et Appliquées, Université Nangui ABROGOUA, 02 BP 801 Abidjan 02, Côte d'Ivoire
[2]Centre de Recherches Océanologiques d'Abidjan, 1071, rue Roger Zinzou, BP V 18 Abidjan, Côte d'Ivoire
[3]Univ. Lille, CNRS, Centrale Lille, Univ. Artois, UMR 8181 - UCCS - Unité de Catalyse et Chimie du Solide, F-59000 Lille, France.
*Corresponding author E-mail: siratasoro36@gmail.com

http://dx.doi.org/10.13005/ojc/420223

(Received: February 21, 2026; Accepted: April 04, 2026)

ABSTRACT

This study focuses on synthesizing and characterizing environmentally friendly and cost-effectiveactivated carbons (AC) using shea nut shells (*Vitellaria paradoxa*). The shells were chemically modified with phosphoric acid (H3PO4) and potassium hydroxide (KOH). The optimization process employed a designed experiment, with the iodine number as the response parameter. The Physicochemical properties like surface morphology, surface charge, thermal stability, and specific surface area, were systematically characteristics. The optimized activated carbons reached a point of zero charge (pHpzc) of 5.73 for ACK-HP600-2 and 6.12 for ACK-HP400-5, showing their acidic nature. X-ray diffraction revealed an amorphous structure, while BET analysis showed specific surface areas of 458.1637 m^2/g for ACK-HP600-2 and 695.3626 m^2/g for ACK-HP400-5. Scanning electron microscopy (SEM) images displayed microporous surfaces with numerous interconnected pores. This research highlights the potential of agricultural waste for economically producing activated carbons, particularly for wastewater treatment applications.

Key words: Characterization, Activated Carbon, Shea Nut Shells, Optimization, Experimental Design.

INTRODUCTION

The world is currently facing major environmental problems related to gaseous, liquid, and solid waste emissions. With technological advances and population growth, waste management has become a critical challenge, particularly in developing countries[2]. While some waste materials decompose naturally, others, which are non-biodegradable or challenging to process, accumulate and contribute to environmental pollution[3]. The processing of agricultural materials, whether artisanal or industrial, generates substantial lignocellulosic residues, which are often disposed of by landfilling or incineration[4]. However, these methods are sometimes unsuitable due to the by-products resulting from their decomposition. To overcome this problem, many researchers worldwide have developed cost-effective activated carbons rom agricultural waste to enhance their utilization[5].

Activated carbons are carbon adsorbents typically synthesized as granular or powdered solids. They are characterized by a highly developed porous architecture and heterogeneous chemical composition6. These materials are widely utilized in diverse industrial applications, including atmospheric filtration systems, water desalination, wastewater remediation, and gold extraction processes[7]. They are not only used as adsorbents, but also as supports for catalysts. Their production can occur through two methods: physical activation or chemical activation[8] K_2CO_3, and simultaneous steam and K_2CO_3 at the temperature of 600 °C. The characterization of the activated biocarbon samples was carried out via several instrumental techniques such as TGA, XRD, FTIR, Raman, and N2 sorption at the temperature of 77 K. The values of the specific surface area, of the prepared activated carbons, determined by means of N2 adsorption measurements were between 5 and 600 m2/g. The CO_2 adsorption equal to 2.63 mmol/g at the pressure of 1 bar and the temperature of 0 °C was achieved. The activated biocarbons produced from olive pomace by combined physical and chemical activation showed considerable promise for flue gas carbon capture applications. The values of adsorption at 0.15 bar were more than 50 % of adsorption at 1 bar pressure for all investigated activated carbons. High selectivity of CO_2 over N2 equal to 29 was achieved for the gas composition of 15 % v/v CO2 and 75 % v/v N2. For CO2 adsorption the small pore volume (diameter ≤0.79 nm for 1 bar and diameter ≤ 0.55 nm for 0.15 bar. Physical activation results from heat treatment and involves two main steps: carbonization or pyrolysis, and followed by activation9. Regarding chemical activation, a diverse range ofreagents including KOH, NaOH, ZnCl2, and H3PO4have been extensively employed as activating agents10. Moreover, the performance of chemically activated carbons surpassed that of physically activated counterparts by a factor of approximately 3.7[11].

The development of high-performance activated carbons from lignocellulosic precursors has been the subject of rigorous investigation, driven by the need for cost-effective and renewable environmental remediation materials[12]. These precursors include corn stalks[13] flash heating was applied for activated carbon (AC, coconut shells14, peanut shells[15], olive pits[16], cola nut shells[17], orange and lemon peels[18] orange and lemon peels-derived activated carbon (OLPAC, Moringa oleifera19, coffee shells[20], wood[21], wheat straw[22], and fruit pits[23]

In this context, the present work aims to promote shea nut shells (Vitellaria paradoxa) into effective activated carbons for environmental remediation[24]. The shea tree is a wild crop that grows naturally[25], and it is particularly valuable for its butter, which has medicinal, nutritional, and cosmetic properties, being relatively widespread across various African countries[26]. The nuts are widely traded and consumed, while the shells often end up in landfills, representing a considerable amount of waste that is difficult to degrade.

This study aims to optimize the synthesis of activated carbons derived from shea nut shells. Utilizing a Design of Experiments (DoE), we systematically refined the production process and subsequently characterized the resulting carbons to evaluate their efficacy for wastewater remediation applications.

MATERIALS AND METHODS

Chemical equipment

The specifications and sources of the reagents used for the synthesis and characterization are summarized in Table 1.

Plant material

Shea nut shells (CK) (Fig. 1) were collected from residues of artisanal processing. The collection site is Talléré, a sub-prefecture in the Korhogo department, located in northern Côte d'Ivoire. To eliminate residual pulp and extraneous impurities, the shea shells underwent multiple rinses with tap water. The cleaned biomass was subsequently dehydrated in a forced-air oven at 105 °C for 24 hours to ensure constant mass. Following dehydration, the samples were comminuted and classified using standard sieves to isolate a particle size fraction between 0.5 and 2 mm. The resulting precursor was stored in hermetically sealed containers to maintain dryness prior to the activation process.

Study methods

Synthesis of activated carbon (AC)

The synthesis of the activated carbon was achieved through a chemical activation protocol[27]characterization, and applications of activated carbons obtained by novel chemical activation with $FeCl_3$. The text includes a description of the activation mechanism, which compromises three different stages: (1. We employed an experimental design framework to systematically investigate the influence of various process parameters. Specifically, a Hadamard matrix, a type of screening design, was utilized for the synthesis of activated carbons. This approach facilitates the rapid identification of significant factors affecting the target variables through a minimized number of experimental trials, making it particularly effective for initial process optimization involving multiple variables. The corresponding linear model is expressed by the following equation:

$$y = b_0 + \sum_{i=0}^{n} b_i X_i \quad \text{....(1)}$$

Where:

b_0: Arithmetic mean of the response

b_i: Regression coefficients associated with each independent factors Xi

y: Represents the experimental response.

The parameters defining the experimental domainare summarized in Table 2.

Table 3 shows the experimental design. For the impregnation process, 20 g of the CK precursorwas submerged in 100 mL of either phosphoric acid (H_3PO_4) or potassium hydroxide (KOH) at the specified concentrations.Following 12 hours of continuous stirring to facilitate the interaction between the activating agent and the CK precursor, the resulting mixture was aged for 24 hours. The solid substrate was subsequently recovered via Büchner funnel filtration and dehydrated in a forced-air oven at 105 °C for 24 hours.

For each sample,the dehydrated precursors were subjected to carbonization within a Nabertherm muffle furnace.The thermal treatment was conducted at specified temperatures utilizing a consistent ramp rate of 5 °C/min. Following calcination, the synthesized activated carbons were cooled and rinsed repeatedly with distilled water.This washing process was maintained until the filtrate achieved a stable pH between 6 and 7. Finally, they were dried again in an oven at 105°C for 24 hours. The activated carbons, produced at 400 °C for 5 hours and at 600 °C for 2 hours, activated by phosphoric acid (H3PO4) or potassium hydroxide (KOH), were designated ACK-HP400-5 and ACK-KH600-2, respectively (Fig. 2). The iodine number was used as a factor of interest.

Iodine Adsorption Capacity (Iodine Number)

The iodine number (I_N) serves as a fundamental metric for characterizing the microporous framework of activated carbons[28]. In this study, the iodine number was determined following a modified protocol based on the methodology established byKonan and Amadou[29,30]. Specifically, 0.05 g of the synthesized activated carbon was equilibrated with 15 mL of a 0.2 N aqueous iodine solution for a duration of 4 minutes. Following this contact period, the suspension was filtered to separate the adsorbent.A 10 mL aliquot of the resulting filtrate was then titrated against a 0.1 N sodium thiosulfate (Na2S2O3.5H2O) titrant.To ensure visual accuracy in determining the equivalence point, a 0.1 N starch solution was employed as a colorimetric indicator. A blank titration, conducted under identical experimental conditions but in the absence of the carbonaceous material, was performed to establish a reference value. The iodine number (), defined as the milligrams of iodine adsorbed per gram of activated carbon (mg/g), was determined according to the followingexpression:

$$I_N = \frac{(V_b - V_s) \times N \times 126.9 \times (\frac{15}{10})}{m} \quad ...(2)$$

Where:
V_b and V_s: Volumes (mL) of sodium thiosulfate solution consumed during the blank titration and sample titration, respectively
N: Normality of the thiosulfate titrant
m: Dry mass (g) of the adsorbent utilized in the procedure

Analytical Characterization of Synthesized Activated Carbons

To elucidate the relationship between synthesis parameters and material performance, a suite ofcomplementary analytical techniques was employed.The structural and chemical properties of the resulting activated carbons were rigorously characterized through a multifaceted analytical framework.

Point of Zero Charge (pH_{pzc})

The point of zero charge (pH_{pzc}) represents the specific pH level at which the net electrical charge on the adsorbent surface is neutralized within an aqueous medium. This parameter was identified using the salt addition method adapted from established protocols[31]. Initially,aseries of beakers were filled with 50 mL of a 0.1 M NaCl solution,with the initial pH (pHi) adjusted between 2 and 11 using micro-addition of 0.1 M NaOH or HCl.

Subsequently, 150 mg of the synthesized activated carbon was introduced into each solution. The resulting suspensions were agitated for 48 hours at ambient temperature to ensure the system reached equilibrium. After this period, the mixtures were filtered, and the equilibrium pH (pH_f) was measured using a calibrated Hanna HI 9813-5 pH meter. The pHpzc was determined by plotting the variance ($\Delta pH = pH_f - pH_i$) against the initial pH values. The pHpzc for each adsorbent was defined as the x-intercept where $\Delta pH = 0$.

Brunauer-Emmett-Teller (BET) Surface Area Analysis

The porous structure of the synthesized materials was characterized using nitrogen (N_2) adsorption-desorption isotherms at 77 K, conducted on a Micromeritics TriStar II Plus analyser. Before measurement, samplesunderwent an overnight degassing process at 300 °C under primary vacuum to eliminate residual moisture. The specific surface area (S_{BET}) was evaluated via the Brunauer-Emmett-Teller (BET) method. Additionally, the total pore volume was derived from the amount of nitrogen adsorbed at a relative pressure (P/P_0) of 0.95, while the micropore volume was quantified using the Dubinin-Astakhov equation.

Where:
P: Equilibrium pressure
P_0: Saturation vapour pressure of the adsorbate

X-Ray Diffraction (XRD) Analysis

The crystalline and amorphous composition of the solid samples was determined through X-ray diffraction (XRD) analysis. It also provides quantitative information on the arrangement of elements in a material, as well as qualitative data for identifying different crystalline compounds and their crystallographic forms.

The XRD analyses were conducted using a Bruker D8 Advanced diffractometer, equipped with a Cu KΔ1 monochromatic radiation source operating at 40 kV and 30 mA. The X-ray diffractograms were obtainedwithin the range of 5 to 60°, recorded with a step size of 0.05° and a step time of 1 second. The analyzed sample and the diffraction signal were recorded according to the following equation:

$$\lambda = 2d \sin(\theta) \quad ...(3)$$

Where:
λ : X-ray source wavelength
d: inter-reticular spacing
θ: glancing diffraction angle (Bragg angle)

Thermal Gravimetric Analysis (TGA)

The thermal properties of activated carbon were studied as a function of temperature using thermogravimetric analysis (TGA). The analysis was conducted under a nitrogen environment, utilizing a constant purge flow of 50 cm3/min. Approximately 10 mg of the activated carbon was heated from 25 to 800 °C. at a linear ramp rate of 10 °C/min.

Scanning Electron Microscopy (SEM) Analysis

Scanning electron microscopy is a powerful analytical technique used for the rapid

characterization of solid-state materials, providing high-resolution images that reveal both surface topology and elemental distribution. A JEOL JSM-7800F scanning electron microscope, operated at 5.00 kV, was employed to evaluate the surface architecture of the adsorbents. A 200 nm carbon film was deposited onto the samples before observation to facilitate electron discharge and improve image clarity.

RESULTS AND DISCUSSION

Optimization of activated carbon preparation

This section examines the critical parameters governing the synthesis of activated carbon to determine their impact on the final product.

Table 4 delineates the specificexperimental design parameters alongside the resulting data for each of the five variables under consideration. Iodine values varied from 159.843 to 414.912 mg/g across the different activation treatments investigated. This iodine number is animportant measure of activated carbon performance, providing an estimate of the total surface area available for adsorbing low-molecular-weight compounds. The best result was obtained in test number 5, with a value of 414.912, comparable to the 446.706 mg/g reported by Dibi32, who used coconut shells as a precursor.

Estimation of various coefficients

The coefficients obtained range from 41.00 to 67.00 for the iodine number. The standard deviations associated with the iodine number are relatively high, reaching 33.125 mg/g. Table 5 presents the computational coefficients generated by the NemrodW 2000software package. Upon replicating the conditions of run 5, the experimental error was quantified, yielding a standard deviation of 33.125. Thus, a coefficient is deemed statistically significant only when its magnitude exceeds twice the estimated experimental error33. Statistical analysis indicates that the activating agent is the only factor with an effect exceeding the experimental error, thereby identifying it as the primary driver of the measured responses.

Table 1: Chemicals used

Chemical	Purity	Sources
Phosphoric acid (H_3PO_4)		
Molar mass = 98.00 g/mol, density = 1.70	85 %	Merck
Potassium hydroxide (KOH)		
Molar mass = 56.11 g/mol	85 %	PanReac AppliChem
Iodine (1,0 N)	-	Prolabo
Hydrochloric acid (HCl)	30 %	Prolabo
Sodium hydroxide (NaOH)	40 %	Prolabo
Sodium thiosulfate ($Na_2S_2O_3$. $5H_2O$)		
Molar mass = 248.18 g/mol	99 %	PanReac AppliChem

Table 2: Experimental domain

Factors	Shea nut shell (CK)	
	-1	+ 1
X1 : Particle size (mm)	0.5	2
X2 : Activating agents	KOH	H_3PO_4
X3 : Concentration (mol/L)	1	3
X4 : Temperature (°C)	400	600
X5 : Time (h)	2	5

The results also show that activation with phosphoric acid generates higher iodine number values than those obtained with potassium hydroxide. Phosphoric acid is acknowledged as the most effective activating agent. It enables the production of high-quality adsorbent and to develop significant porous structures with large specific surface areas20. The activated carbons with the best properties were obtained in tests 2 and 5. These two samples, designated ACK-HP600-2 and ACK-

HP400-5, respectively, were selected for this study.
Surface Area Analysis

Activated carbons derived from shea nut shells (Vitellaria paradoxa), prepared under optimal conditions taking into account the iodine number, were subjected to thorough characterization. Figure 3 illustrates the nitrogen (N2) adsorption and desorption isotherms for the optimal activated carbons at 77 K. According to the classification by the International Union of Pure and Applied Chemistry (IUPAC)[34], the nitrogen adsorption and desorption isotherms are classified as type I. They show a significant increase in adsorption at low P/P0 values (< 0.1), with a slightly marked inflection and a long plateau parallel to the P/P0 ≈ 1.0 axis. This observation indicates a microporous structure of the prepared activated carbons, with minimal or no mesoporosity[35].

In this study, although the adsorption and desorption isotherms are similar for the two samples, significant variations in adsorption capacities are observed depending on the H_3PO_4 concentration. Indeed, an increase in this concentration causes an upward shift in the isotherm compared to the other carbon. The impact of acid concentration on the porosity and surface area metrics (BET, micropore, and mesopore volumes) of the optimal activated carbons is documented in Table 6. The cumulative pore volume was determined at a relative pressure of 0.95, representing the volume of nitrogen condensed within the pores in its liquid state[36]. Microporosity was quantified using the Dubinin-Astakhov model, whereas the mesopore contribution was determined by subtracting the micropore volume from the cumulative pore volume. Data reveal that increasing the acid concentrationsystematically elevates the BET surface area and total pore capacity.Such

Table 3: Experimental design

Exp.	Particle size (mm)	Activating agent	Concentration (mol/L)	Carbonization temperature (°C)	Carbonization time (h)
1	2	H_3PO_4	3	400	5
2	0.5	H_3PO_4	3	600	2
3	0.5	KOH	3	600	5
4	2	KOH	1	600	5
5	0.5	H_3PO_4	1	400	5
6	2	KOH	3	400	2
7	2	H_3PO_4	1	600	2
8	0.5	KOH	1	400	2

Table 4: Experimental responses

Test	Particle size (mm)	Activating Agent	Concentration (mol/L)	Carbonization temperature (°C)	Carbonization time (h)	Response Iodine number (mg/g)
1	2	H_3PO_4	3	400	5	255.069
2	0.5	H_3PO_4	3	600	2	312.884
3	0.5	KOH	3	600	5	351.995
4	2	KOH	1	600	5	159.843
5	0.5	H_3PO_4	1	400	5	414.912
6	2	KOH	3	400	2	295.880
7	2	H_3PO_4	1	600	2	295.880
8	0.5	KOH	1	400	2	255.069

temperature-dependent porosity development arises from impregnation with phosphoric acid, which inhibits tar formation and promotes the release of volatile materials, thereby creating more micropores[37]. These findings align with the observations from other researchers[38,] who established that augmentingthe phosphorus content serves to enhance the cumulative volume ofthe micropores. Furthermore, the experimental results presented in Table 6demonstrate a positive correlation between H_3PO_4 loading and average pore diameter, implying that higher acid concentrations facilitate both the creation of new voids and the broadening of the established pore structure. Comparableimpacts of phosphoric acidconcentration on porosity development have been perceived in other lignocellulosic precursors[39].

Point of Zero Charge (pH_{pzc})

The point of zero charge (pHpzc)represents the specific pH threshold at which the adsorbent's surface maintains a neutral net electrical charge. Figure 4 shows the pH_{pzc} values, 5.73 for ACK-HP600-2 and 6.12 for ACK-HP400-5, indicating

Table 5: Estimation of the different coefficients

	b_0	b_1	b_2	b_3	b_4	b_5	Experimental error (Se)
Iodine number	290.00	- 41.00	67.00	11.250	-12.750	2.750	33.125

Table 6: Pore structure parameters of activated carbons from shea nut shells

	Specific surface (m^2/g)	Average pore diameter (nm)	Total pore volume(cm^3/g)	Micropore volume (cm^3/g)	Mesopore volume (cm^3/g)
ACK-HP400-5	458.1637	1.8202	0.213074	0.190383	0.022691
ACK-HP600-2	695.3626	1.8833	0.323914	0.279017	0.044897

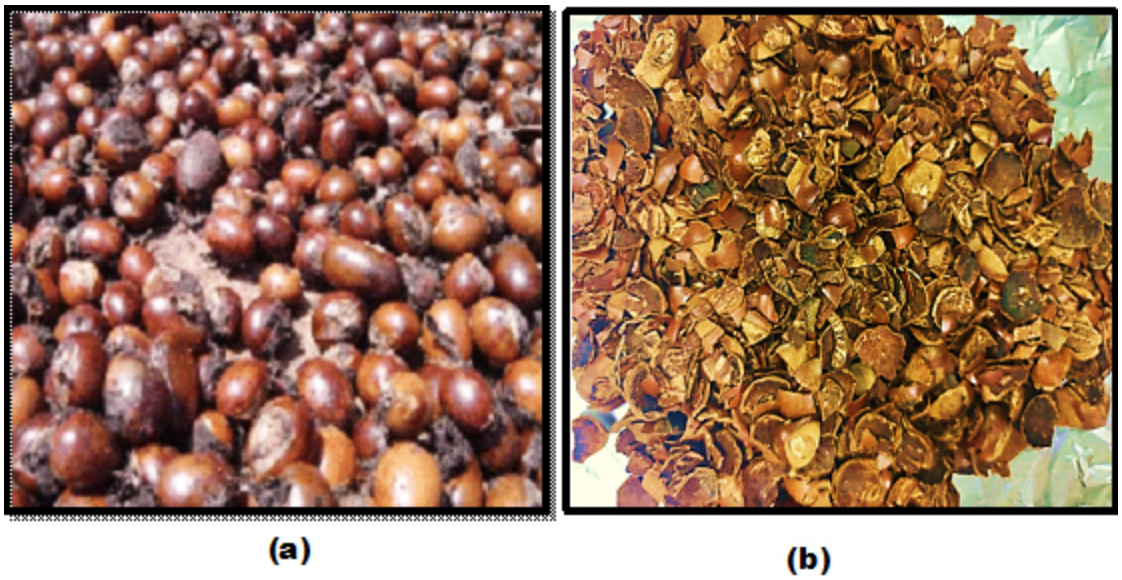

Fig. 1. Photographic representation of shea (Vitellaria paradoxa) components: (a) whole nuts, (b) recovered nut shells(Source: Study's photo)

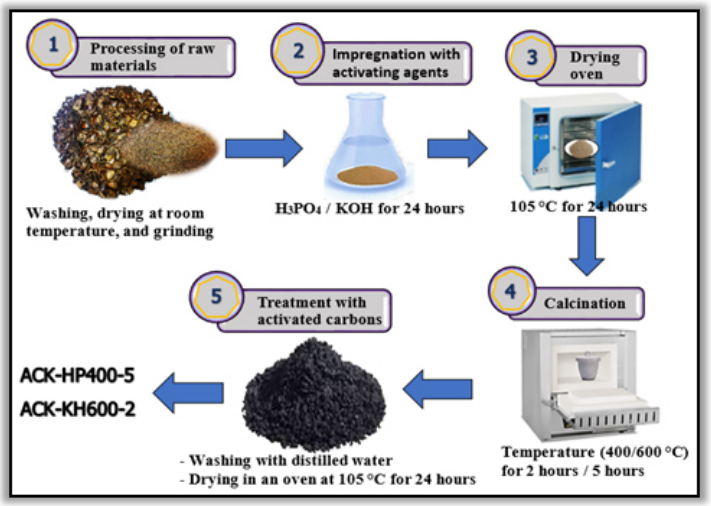

Fig. 2. Scheme of synthesis protocol for shea nut shells-derived activated carbons. (This work)

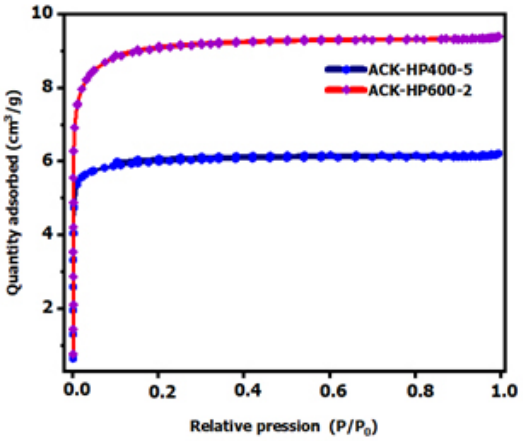

Fig. 3. N2 adsorption and desorption isotherms of optimal activated carbons

that both activated carbons are acidic. These pH values correspond to the conditions under which both carbons exhibit electric potential neutrality. This suggests that at solution where pH > pH_{pzc},the adsorbent surface undergoes deprotonation, creating a negative net charge that facilitates the electrostatic attraction of cationic species. In contrast, at pH < pH_{pzc}, surface protonation yields a positive charge, thereby enhancing the affinity for anionic pollutants through favourable coulombic interactions[33].

X-Ray Diffraction (XRD)Analysis

Figure 5 illustrates the diffractograms of the optimized activated carbons, ACK-HP600-2 and ACK-HP400-5.These data elucidate the fundamental structural characteristics of the adsorbents produced from shea nut shells precursors. These activated carbons, derived from shea nut shells (*Vitellaria paradoxa*), each exhibit two large significant peaks in the 2Δranges of 20 to 30° and 40 to 50°, with maximum intensities around 25° and 43°, respectively.The absence of sharp peaks in activated carbon (AC) indicates a mainly amorphous structure. It is evident that these materials have a high carbon content, whichis typical of adsorbent materials. This feature is typical of chemically activated carbons, where activation by H3PO4 promotes the formation of a porous network while reducing the crystallinity of the initial material, as demonstrated by Alvez-Tovar and Jahan[5,40]. Under the effect of activation and increased temperature, a disordered structure allows for the formation of a highly developed porous structure, which is essential for the effectiveness of activated carbons.

Similar results have been reported by other researchers, such as Ramutshatsha-Makhwedzha and Charmas, concerning the production of activated carbon from agricultural waste[18,41]. These studies confirm that amorphous morphology is advantageous for promoting pore creation during the activation process.

Thermal Gravimetric Analysis (TGA)

The thermal stability of the shea nut shell activated carbon was evaluated via TGA/DTG analysis, as depicted in Figure 6. The curves delineate the stages of mass loss as the system was heated from ambient conditions to a maximum of 900 °C. The thermogravimetric profile reveals three well-defined degradation phases. An initial endothermic event is observed between 30 °C and 170 °C, reaching its maximum intensity at 100 °C (figures 6a and 6b); this transition is primarily associated with the desorption of physically bound water. This water comes from the H_3PO_4 solution, the moisture contained in the samples, and interactions between the samples and H_3PO_4 at low temperatures. At this stage, it is also possible to release volatile components and light gases such as CO and CO_2. The second stage is characterized by rapid degradation observed during 170 °C and 500 °C, marked by a greater loss of mass. Previous studies have demonstrated that this phase corresponds to the thermal decomposition of lignocellulose, including hemicellulose and cellulose[42]. Finally, the third stage, which begins above 500°C, is characterized by the consolidation of the carbon structure, with low-intensity peaks leading to a decrease in mass loss due to lignin decomposition. This phase can be attributed to the final oxidation of the carbonaceous material following its reaction with H_3PO_4. Similar observations have been reported for other activated carbons, such as castor bean residues[43] and Jatropha curcas fruit shells[44].

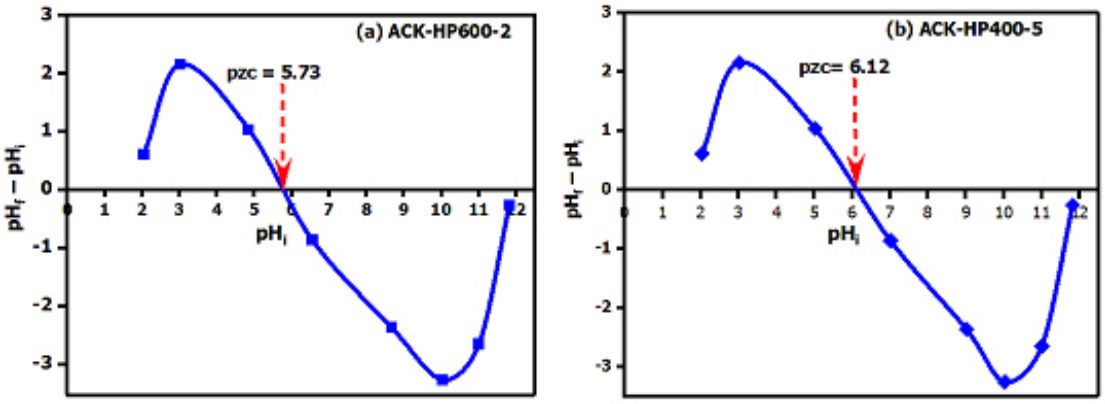

Fig. 4. pH_{pzc} of optimal activated carbons: a) ACK-HP600-2 b) ACK-HP400-5

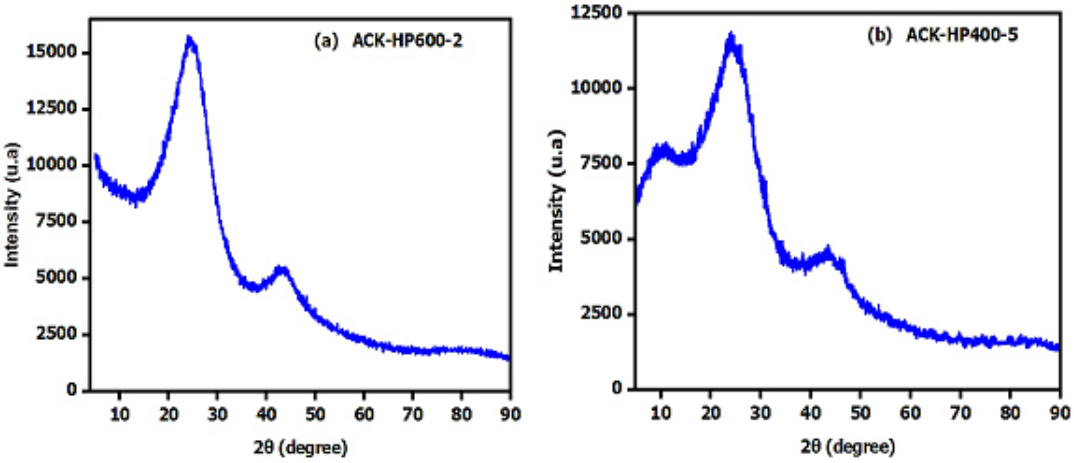

Fig. 5. XRD of optimal activated carbons: (a) ACK-HP600-2 and (b) ACK-HP400-5

Scanning Electron Microscopy (SEM) Analysis

The surface morphology of the synthesized adsorbents is presented in Figure 7,depicting a series of activated carbons characterized by highly heterogeneous and rugose architectures. Micrographs obtained via scanning electron microscopy (SEM) for the ACK-HP600-2 sample (figures 7a and 7b) demonstrate a prolific development of macroporous networks and deep interstitial cavities, indicating a high degree of structural maturation during the activation process. This porous development is probably attributed to the evaporation of phosphoric acid (H3PO4), thus freeing up previously occupied spaces. Njewa demonstrated that adequate amounts of phosphoric acid, combined with an appropriate activation temperature, produce activated carbon with a large specific surface area and an optimized porous structure[12]. In contrast, ACK-HP400-5 carbon has cavities on its surface and a reduced pore volume, taking the form of slits, which makes it less porous compared to the other carbon. The surface of ACK-HP400-5 shows white particles and impurities formed due to the presence of H^3PO^4. This suggests that the acid has induced

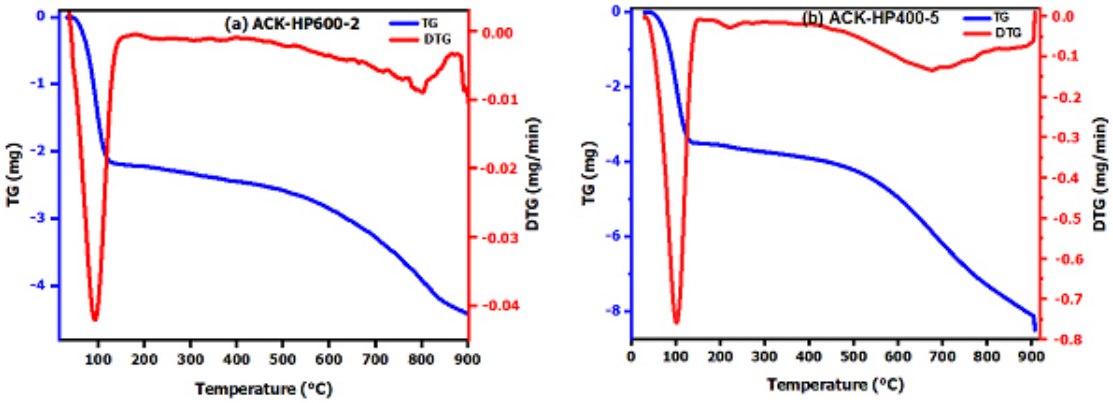

Fig. 6: TGA/DTG of activated shea nut shells: (a) ACK-HP600-2, (b) ACK-HP400-5

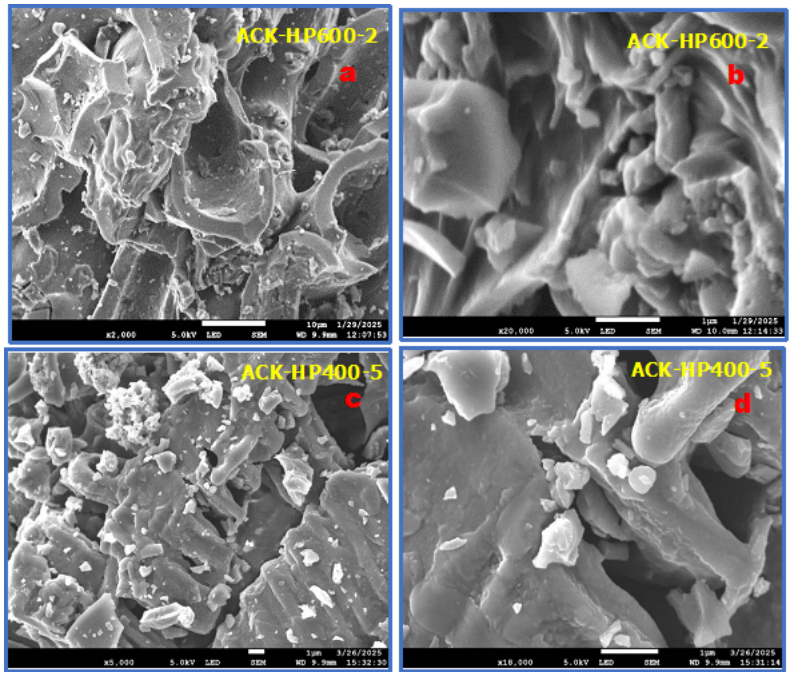

Fig. 7. SEM images of optimal activated carbons: ACK-HP600-2 (a, b) and ACK-HP400-5 (c, d)

cracks on the surface of the activated carbon (figures 7c and 7d). These observations are consistent with the results of analyses conducted by Mekuiko[45].

CONCLUSION

The synthesis of activated carbon from shea nut shells was optimized through chemical activation with KOH and H_3PO_4, guided by a systematic Hadamard experimental framework. It was observed that the concentration of the activating agent, whether KOH or H3PO4, significantly influences the iodine number. This study demonstrated that the carbons activated with phosphoric acid, particularly ACK-HP600-2 and ACK-HP400-5, yield better results compared to those activated with potassium hydroxide. Phosphoric acid is therefore recognized as the superior activating agent. The activated carbons prepared in this way have large specific surface areas of 695.362 m²/g for ACK-HP600-2 and 458.163 m²/g for ACK-HP400-5. The chemical activation of this material has generated active microporous sites, corresponding to type I isotherms. The characteristics of these carbons also revealed their acidic nature. Subsequent investigations will systematically evaluate the adsorption performance of these functionalized carbons against a diverse array of contaminants to determine their practical utility in wastewater remediation. This study highlights the potential of shea nut shell derived activated carbons as a viable feedstock for engineering sustainable technologies aimed at mitigating modern environmental issues.

ACKNOWLEDGEMENTS

The authors are gratefulto Nangui ABROGOUA University and its Central Laboratory for providing the essential technical facilities and support that made this research possible.

Conflict of Interest

The authors declare that they have no known competing financial interests or personal relationships that could have appeared to influence the work reported in this manuscript.

Funding Sources

The authors declare that this study was self-funded and did not receivegrants or financial backing from any third-party sources.

Data Availability Statement

Supporting data for the findings of this research are maintained by the authors and may be released upon request.

Ethical Approval Statement

The authors collectively affirm their consent for the publication of this research in its entirety.

Informed Consent Statement

All listed authors have reviewed the manuscript and approve its submission to this journal.

Authors' Contributions

Sirata Ibrahima FrancisSORO: Original draft preparation, Writing, Data curation, Software, Visualization

Affoué Tindo SylvieKONAN

Writing, Formal analysis, Software

Ignace ChristianM'BRA

Writing, Original draft preparation, Visualization

koffi SiméonKOUADIO

Review and editing, Formal analysis, Visualization

Tanoé Lucien AKETCHI

Investigation, Visualization

Daniel YannickDJÈ: Investigation

LyndaEKOU: Conceptualization, Methodology

TchiriouaEKOU: Supervision, Validation

REFERENCES

1. Zuhara, S.; McKay, G., *J. Environ. Chem. Eng.,* **2024**, *12*, 112836.
2. Charmas, B.; Zi&xio, M.; Jedynak, K.; Kucio, K., *J. Therm. Anal. Calorim.,* **2023**, *148*, 7403–7419.
3. Bouzid, T.; Grich, A.; Naboulsi, A.; Regti, A.; Alaoui Tahiri, A.; El Himri, M.; El Haddad, M., *Inorg. Chem. Commun.,* **2023**, *158*, 111544.

4. Metyouy, K.; Benkirane, L.; Sánchez, M.E.; Cara-Jiménez, J.; Plakas, KV.; Chafik, T., *Sustain. Chem. Environ.,* **2024**, *6*, 100110.
5. Alvez-Tovar, B.; Scalize, P.S.; Angiolillo-Rodríguez, G.; Albuquerque, A.; Ebang, M N.; De Oliveira, T.F.,*Sustain.*,**2025**, *17*, 1–25.
6. Cano, F. J.; Reyes-Vallejo, O.; Sanchez-Albores, R. M.; Sebastian, P. J., *Sustainability,* **2025**, *17*, 1–23.
7. Abdulkarim, M.; Ibrahim, I. L.; Mohammed, M.; Musah, M., *FUDMA J. Sci.,* **2024**, *8*, 409–415.
8. Kiełbasa, K.; Bayar, Δ; Varol, EA.; SreΔscek-Nazzal, J.; Bosacka, M.; Michalkiewicz, B.,*Ind. Crops Prod.,* **2022**, *187*, 115416.
9. Tapia, Y. M.; De Oliveira, T. F.; Gabriel, E. F. M., *Rev. Gest. Soc. E Ambient.*, **2023,** *17*, 1–19.
10. Mfoumou, C. M. Mbouiti, B. L.; Mougnala, S.B.; Tonda-mikiela, P.; Tchouya, G. R. F., *Open J. Inorg. Chem.,* **2024**, *14*, 19–32.
11. Kra, D.O.; Allou, N.B.; Atheba, P.; Drogui, P.; Trokourey, A., *J. Encapsulation Adsorpt. Sci.,* **2019**, *9*, 63–82.
12. Njewa, J.B.; Vunain, E.; Biswick, T.*, J. Chem.,* **2022**, *1*, 9975444.
13. Yurtay, A.; Kılıç, M., *Diam. Relat. Mater.,* **2023**, *131*, 109603.
14. Singla, M. K. Gupta, J.;Safaraliev, M.; Nijhawan, P.; Oberoi, A. S.; Menaem, A., *Int. J. Hydrogen Energy,* **2024**, *61*, 1417–1428.
15. Zhan, Y.; Zhou, H.; Guo, F.; Tian, B.;Du, S.; Dong, Y.; Qian, L.,*J. Energy Storage,* **2021**, *34*, 102180.
16. Saleem, J.; Shahid, U.B.; Hijab, M.; Mackey, H.; McKay, G., *Biomass Convers. Biorefinery,* **2019**, *9*, 775–802.
17. Idris-Hermann, K.T.; Raoul, T.T.D.; Giscard, D.; Gabche, A.S*., Chem. Sci. Int. J.*,**2018**, *23*, 1–15.
18. Ramutshatsha-Makhwedzha, D.; Mavhungu, A.; Moropeng, M.L.; Mbaya, R., *Heliyon,* **2022**, *8*, e09930.
19. Raji, Y.; Nadi, A.; Mechnou, I.; Saadouni, M.; Cherkaoui, O.; Zyade, S.,*Diam. Relat. Mater.,* **2023**, *135*, 109834.
20. ZiΔzio, M.; Charmas, B.; Jedynak, K.; Hawryluk, M.; Kucio, K., *Appl. Nanosci.,***2020**, *10*, 4703–4716.
21. Mohamad Yusop, M.F.; Nasehir Khan, M.N.; Zakaria, R.; Abdullah, A.Z.; Ahmad, M.A., *Arab. J. Chem.,* **2023**, *16*, 104780.
22. Agarwal, S.; Singh, A.P.; Mathur, S*., Environ. Sci. Pollut. Res.,* **2023**, *30*, 41073–41094.
23. Khan, T.A.; Nouman, M.; Dua, D.; Khan, S.A.; Alharthi, S.S., *J. Saudi Chem. Soc.,* **2022**,*26*, 101417.
24. Musah, M., *FUDMA J. Sci.*,**2024**,*8*, 338–344.
25. Balogun, O.S.; Aasa, O.,*FUDMA J. Sci.*,**2019**, *3*, 381–386.
26. Kareem, I.A.; Sanni-Bamigbade, S.A.; Adekola, O.A.; Abioye, T.M.,*FUDMA J. Sci.,* **2025**, *9*, 369–374.
27. Bedia, J.; Peñas-Garzón, M.; Gómez-Avilés, A.; Rodriguez, J. J.; Belver, C., *J. Carbon Res.,* **2020**, *6*, 1–25.
28. Mamane, O.S.; Zanguina, A.; Daou, I.; Natatou, I., J. la Société ouest-Africaine Chim., **2016**, *41*, 59–67.
29. Konan, A.T.S.; Richard, R.; Andriantsiferana, C.; Yao, K. B.; Manero, M.H., *J. Mater. Environ. Sci.,* **2020**, *11*, 1584–1598.
30. Amadou Kiari, M.N.; Konan, A.T.S.; Sanda Mamane, O.; Kone, H.; Fanou, G.D.;Siragi Dounounou Boukari, M.; Ibrahim Grema, M.H.;Malam Alma, M.M.;Yao, K.B., *Mater. Sci. Forum.*, **2024**, *1122*, 91–98.
31. Yannick, D.D.; Zoungranan, Y.; Dobi-Brice, K.K.; Lynda, E.; Tchirioua, E., *Sci. J. Chem.,* **2023**, *11*, 189–196.
32. Dibi, K.; Meite, L.; Aboua, N.K.; Soro, B.D.; Kossonou, R.G.; Traore, K.S.; Konan, G.; Mamadou, K.,*Int. J. Innov. Appl. Stud.,***2021**, *33*, 214–221.
33. Armand, A.E.; Augustin, Y.Y.; Urbain, K.Y.; Albert, T., *Int. J. Innov. Appl. Stud.,* **2020,** *29*, 1161–1171.
34. Bilias, F.; Sewu, D.D.;Woo, S.H.; Anastopoulos, I., *Pure Appl. Chem.,***2024**, *96*, 1541–1572.
35. Yaman, M.; Demirel, M.H., Pollution., **2020**, *6*, 935–944.
36. Brunauer, S.; Emmett, P.H.; Teller, E., Contrib. from Bur. Chem. soils Georg. *Washingt. Univ.,***1938**, *60*, 309-319.
37. Zakaria, R.; Jamalluddin, N.A.; Abu Bakar, M.Z. *Results Mater.* **2021**,*10*, 100183.
38. Du, H; Cheng, J.; Wang, M.; Tian, M.; Yang, X.; Wang, Q.,*Diam. Relat. Mater.,* **2020**,*102*, 107646.
39. Neme, I.; Gonfa, G.; Masi, C., *Heliyon.*,**2022**, *8*, e11940.
40. Jahan, R.A.; Hassan, M.M.; Rana, A.A.;

Karim, M.M.*, Adv. Chem. Eng. Sci.,***2023**, *13*, 189–202.
41. Charmas, B.; Zi⁄xio, M.; Tomaszewski, W.; Kucio, K., Colloids Surfaces A *Physicochem. Eng. Asp.,***2022**, *645*, 128889.
42. El Mansouri, F.; Pelaz, G.; Morán, A.; Da Silva, J.C.G.; Cacciola, F.; El Farissi, H.; Tayeq, H.; Zerrouk, M.H.; Brigui, J., *Separations*., **2022**, *9*, 1-19.
43. Neme, I.; Gonfa, G.; Masi, C., Results Mater., **2022**, *15*, 100304.
44. Tongpoothorn, W.; Sriuttha, M.; Homchan, P.; Chanthai, S.; Ruangviriyachai, C., *Chem. Eng. Res. Des.,* **2011**, *89*, 335–340.
45. Mekuiko, A.Z.; Tchuifon, D.R.T.; Kouteu, P.A.N.; Fotsop, C.G.; Ngakou, C.S.; Kuete, H.I.T.; Bopda, A.; Tamo, A.K.; Anagho, S.G.*,Desalin. Water Treat.*, **2023**, *300*, 144–157.